Spherical near field acoustic holography with microphones on a rigid sphere

Finn Jacobsen[a], Jørgen Hald[b], Efrén Fernandez[a] and Guillermo Moreno[a]

[a]Acoustic Technology Department, Technical University of Denmark, Ørsted Plads, B352, DK-2800 Lyngby, Denmark
[b]Brüel & Kjær Sound & Vibration Measurement A/S, Skodsborgvej 307, DK-2850 Nærum, Denmark
fja@oersted.dtu.dk

Spherical near field acoustic holography (SNAH) is a recently developed technique that makes it possible to reconstruct the sound field inside and just outside an acoustically transparent spherical surface on which the sound pressure is measured with an array of microphones with negligible scattering. Because of the versatile geometry of a sphere SNAH is potentially extremely useful for source identification. On the other hand a rigid sphere is somewhat more practical than an open sphere, and it is possible to modify the SNAH theory so that a similar sound field reconstruction can be made with an array of microphones flush-mounted on a rigid sphere. However, this approach is only valid if it can be assumed that the sphere has a negligible influence on the incident sound field, in other words if multiple scattering can be ignored, and this is not necessarily a good assumption when the sphere is close to a radiating surface. This paper describes the modified SNAH theory and examines the method through simulations.

1 Introduction

Microphone arrays can be used for numerous purposes, e.g., speech enhancement [1], noise mapping and source identification [2], determination of room acoustic parameters [3, 4], and recording of sound [5]. Microphone arrays can have any shape, but in the last few years spherical microphone arrays have been used increasingly. The microphones of a spherical array can be distributed inside an acoustically transparent sphere [6], placed on the surface of an acoustically transparent sphere [3], or flush-mounted on a solid, rigid sphere [4]. Microphone arrays with this geometry have several attractive features. For example, it is obvious that a beamformer based on a spherical microphone array with a high density of the transducers will have essentially the same angular resolution in all directions.

The applications mentioned above are forward problems. For example, beamforming usually takes place far from the sources under examination, and the purpose is to map the far field. However, spherical microphone arrays can also be used for near field acoustic holography, that is, for reconstructing the sound field between the array and the source [7]. This is an inverse problem, and here the spherical array has the significant advantage compared with conventional planar arrays that the usual problem of a finite measurement aperture is nonexistent.

The investigation recently described by Williams et al. [7] was based on an open (transparent) sphere. However, a rigid sphere is somewhat more practical than an open sphere. To this can be added the fact that the boundary conditions are better defined, since it is unlikely that an arrangement with, say, fifty microphones with preamplifiers and cables placed relatively close to each other would not disturb the sound field, as assumed in Ref. [7]. Moreover, it has recently been demonstrated that a rigid sphere is advantageous compared with a transparent sphere (quite apart from the problem of scattering) in beamforming [8]. There might be a similar advantage in spherical near field acoustic holography (SNAH). Anyway, it would be practical if the same spherical array could be used both for beamforming and for near field acoustic holography. On the other hand there is a serious potential problem in mounting the microphones on a solid sphere: in near field acoustic holography the measurement array is always placed fairly near the source under test, because otherwise the evanescent waves will have died out and cannot be reconstructed near the source. The waves that are backscattered from the sphere are likely to be reflected by the surface of the source, and thus they may modify the incident field; and there is no way to distinguish between the original sound field and such reflections. This problem can be expected to depend on the frequency, on the size of the sphere, and on the shape of the source.

This paper examines SNAH based on a solid sphere by a simulation study.

2 Outline of theory

The theory is a fairly straightforward extension of the theory recently presented by Williams et al. [7]. Obviously, the rigid sphere gives rise to scattering, and therefore the total sound pressure is the sum of the incident (that is, undisturbed) sound pressure and the scattered sound pressure,

$$p_{\text{tot}} = p_{\text{i}} + p_{\text{s}} \,. \tag{1}$$

Both the incident and the scattered pressure must be described in terms of solutions to the Helmholtz equation in a spherical coordinate system with the origin at the centre of the sphere. Thus the angular variations of the two components must be described in terms of 'spherical harmonics' [9], that is, in terms of the form

$$\mathrm{Y}_n^m(\theta,\varphi) = \sqrt{\frac{(2n+1)}{4\pi}\frac{(n-m)!}{(n+m)!}}\mathrm{P}_n^m(\cos\theta)\mathrm{e}^{-\mathrm{j}m\varphi} \,, \tag{2}$$

in which P_n^m is an associated Legendre function [9]. The radial dependence of the incident pressure must be described in terms of spherical Bessel functions (j_m) that remain finite also at the origin of the coordinate system, but the scattered pressure, which obviously exists only outside the sphere, should be described in terms of spherical Hankel functions (h_n). The Hankel functions should describe an outgoing field, and are therefore of the second kind because of the sign convention used in this paper ($\mathrm{e}^{\mathrm{j}\omega t}$). It follows that the incident and scattered pressure can be written

$$p_{\text{i}}(r,\theta,\varphi) = \sum_{n=0}^{\infty}\sum_{m=-n}^{n} A_{mn}\,\mathrm{j}_n(kr)\mathrm{Y}_n^m(\theta,\varphi)\mathrm{e}^{\mathrm{j}\omega t} \,, \tag{3}$$

$$p_{\text{s}}(r,\theta,\varphi) = \sum_{n=0}^{\infty}\sum_{m=-n}^{n} C_{mn}\,\mathrm{h}_n(kr)\mathrm{Y}_n^m(\theta,\varphi)\mathrm{e}^{\mathrm{j}\omega t} \,, \tag{4}$$

Because the sphere is rigid the normal component of the particle velocity and thus the gradient of the total pressure vanishes on its surface,

$$\left.\frac{\partial p_{\text{tot}}}{\partial r}\right|_{r=a} = p'_{\text{tot}}(a,\theta,\varphi) = 0 \,. \tag{5}$$

It follows that

$$A_{mn}\,\mathrm{j}'_m(ka) + C_{mn}\,\mathrm{h}'_n(ka) = 0 \,. \tag{6}$$

The amplitudes of the scattered waves can now be described in terms of the amplitudes of the incident waves, and the expression for the total sound pressure becomes

$$p_{\mathrm{tot}}(r,\theta,\varphi) = \sum_{n=0}^{\infty}\sum_{m=-n}^{n} A_{mn}\left(\mathrm{j}_n(kr) - \frac{\mathrm{j}_n'(ka)}{\mathrm{h}_n'(ka)}\mathrm{h}_n(kr)\right)\mathrm{Y}_n^m(\theta,\varphi)\mathrm{e}^{\mathrm{j}\omega t}. \quad (7)$$

Thus the total sound pressure on the surface of the sphere is

$$p_{\mathrm{tot}}(a,\theta,\varphi) = \sum_{n=0}^{\infty}\sum_{m=-n}^{n} A_{mn}\left(\mathrm{j}_n(ka) - \frac{\mathrm{j}_n'(ka)}{\mathrm{h}_n'(ka)}\mathrm{h}_n(ka)\right)\mathrm{Y}_n^m(\theta,\varphi)\mathrm{e}^{\mathrm{j}\omega t}. \quad (8)$$

If this is multiplied with a complex conjugated spherical harmonic and integrated over the whole solid angle then, because of the orthogonality of the spherical harmonics [9],

$$\int_0^{2\pi}\int_0^{\pi} \mathrm{Y}_n^m(\theta,\varphi)\mathrm{Y}_\nu^\mu(\theta,\varphi)^* \sin\theta\, \mathrm{d}\theta\, \mathrm{d}\varphi = \delta_{n\nu}\delta_{m\mu}, \quad (9)$$

the corresponding unknown coefficient A_{mn} results,

$$A_{mn} = \frac{\int_0^{2\pi}\int_0^{\pi} p_{\mathrm{tot}}(a,\theta,\varphi)\mathrm{Y}_n^m(\theta,\varphi)^*\,\mathrm{e}^{-\mathrm{j}\omega t}\sin\theta\,\mathrm{d}\theta\,\mathrm{d}\varphi}{\mathrm{j}_n(ka) - \frac{\mathrm{j}_n'(ka)}{\mathrm{h}_n'(ka)}\mathrm{h}_n(ka)}. \quad (10)$$

Once the coefficients have been determined the incident sound pressure follows from Eq. (1).

The incident particle velocity can also be determined,

$$u_{\mathrm{i},r}(r,\theta,\varphi) = \frac{\mathrm{j}}{\rho c}\sum_{n=0}^{\infty}\sum_{m=-n}^{n} A_{mn}\mathrm{j}_n'(kr)\mathrm{Y}_n^m(\theta,\varphi)\mathrm{e}^{\mathrm{j}\omega t}, \quad (11)$$

$$u_{\mathrm{i},\theta}(r,\theta,\varphi) = \frac{\mathrm{j}}{\rho c}\sum_{n=0}^{\infty}\sum_{m=-n}^{n} A_{mn}\frac{\mathrm{j}_n(kr)}{kr}\frac{\partial \mathrm{Y}_n^m(\theta,\varphi)}{\partial\theta}\mathrm{e}^{\mathrm{j}\omega t}, \quad (12)$$

$$u_{\mathrm{i},\varphi}(r,\theta,\varphi) = \frac{1}{\rho c}\sum_{n=0}^{\infty}\sum_{m=-n}^{n} A_{mn}\frac{\mathrm{j}_n(kr)}{kr}\frac{m\mathrm{Y}_n^m(\theta,\varphi)}{\sin\theta}\mathrm{e}^{\mathrm{j}\omega t}. \quad (13)$$

Finally the incident sound intensity can be calculated from the sound pressure and the particle velocity in the usual way,

$$\mathbf{I}_{\mathrm{i}} = ½\,\mathrm{Re}\left\{p_{\mathrm{i}}\mathbf{u}_{\mathrm{i}}^*\right\}. \quad (14)$$

To summarise, if the sound pressure is known on the surface of a rigid sphere then the entire incident sound field can, at least in principle, be reconstructed.

In practice one obviously cannot expect perfect reconstruction. Inside the sphere the problem is a forward one, but outside the sphere the problem is an ill-posed inverse one. Besides, the sums must obviously be truncated. Moreover, the sound pressure is only known at a finite number of discrete positions. Thus, in practice the coefficients A_{mn} are determined by numerical quadrature.

3 Reflection of the scattered field

As mentioned in the foregoing there is a potential problem in the use of a solid sphere for SNAH: the sound field scattered back towards the source by the sphere will be reflected by the source and thus change the incident sound field. Obviously the reflection depends on the shape and size of the source. However, a point driven simply supported baffled vibrating panel might be a suitable test case. The panel can be modelled with a conventional modal sum; the sound field generated by the panel can be calculated using a numerical approximation to Rayleigh's first integral [9], i.e. by replacing the panel with a collection of monopoles; and the reflections of the backscattered field can be taken into account by introducing an image sphere behind the panel. The image sphere scatters the sound emitted by the monopoles, and the (primary) sphere will be exposed to the direct sound field and to the sound field scattered back from the image sphere.

4 Results

In the following preliminary simulation study there are 50 microphones flush-mounted on a sphere of radius a = 9.75 cm. These microphones are assumed to measure the sound pressure at discrete positions on the sphere, and these positions and the weights used in the numerical integration are taken from the literature [10]. The resulting numerical integration is exact for products of spherical harmonics up to order N = 5, and therefore the sum over n is truncated at this value. Apart from the smoothing caused by this truncation no further regularisation is attempted.

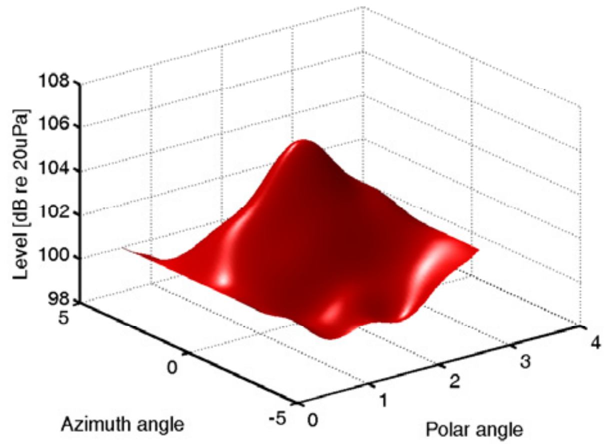

Fig. 1. Sound field generated by a monopole at a distance of 40 cm from the centre of the sphere at ka = 1. Reconstructed sound pressure on a concentric spherical surface of radius 15 cm.

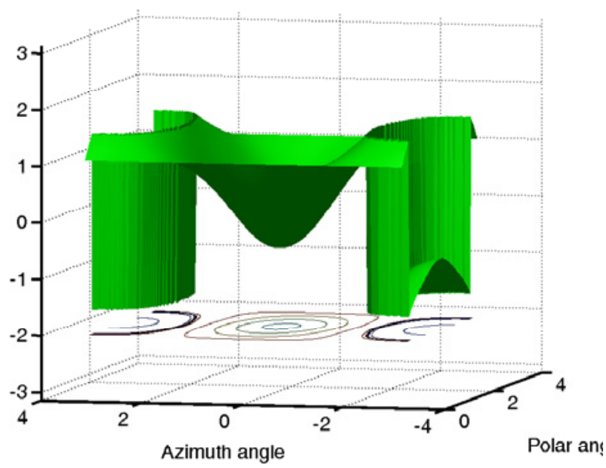

Fig. 2. Sound field generated by a monopole at a distance of 40 cm from the centre of the sphere at ka = 1. Phase of reconstructed sound pressure on a concentric spherical surface of radius 15 cm.

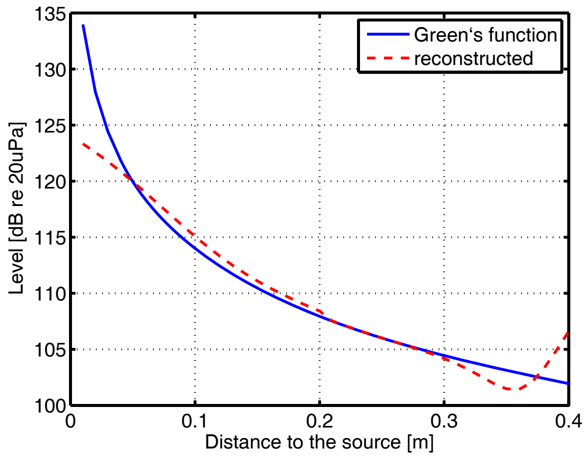

Fig. 3. Sound field generated by a monopole 20 cm from the centre of the sphere at $ka = 2$. 'True' and reconstructed sound pressure along a line through the monopole and the centre of the sphere.

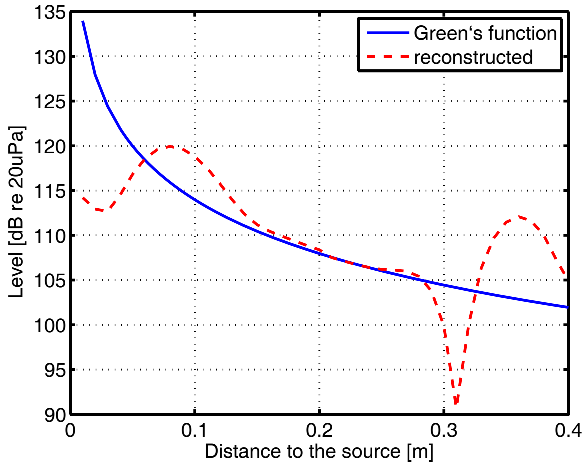

Fig. 4. Sound field generated by a monopole 20 cm from the centre of the sphere at $ka = 5$. 'True' and reconstructed sound pressure along a line through the monopole and the centre of the sphere.

Figure 1 shows an example of reconstruction of the sound pressure amplitude generated by a monopole 40 cm from the centre of the spherical microphone array on a concentric spherical surface with a radius of 15 cm, that is, 5 cm from the surface of the rigid sphere. The frequency corresponds to $ka = 1$. Figure 2 shows the corresponding phase (with phase jumps of π).

Figure 3 shows the result of a similar test case, although here the monopole is 20 cm from the centre of the array and the frequency corresponds to $ka = 2$. As can be seen the reconstruction is very good inside the sphere (from 0.1 to 0.3 m), in particular in the direction away from the source, but the accuracy deteriorates outside the sphere when the distance to the surface exceeds 5 cm. Very similar results have been obtained at lower frequencies (not shown). However, the results shown in Fig. 4, which corresponds to $ka = 5$, demonstrate that reconstruction is unacceptable outside the sphere at such high frequencies.

Figures 5 and 6 show the result when the monopole that generates the sound field is more distant. In this case the monopole is 1 m from the centre of the array. It is apparent that the reconstruction is acceptable at a distance of up to 10 cm from the surface of the sphere.

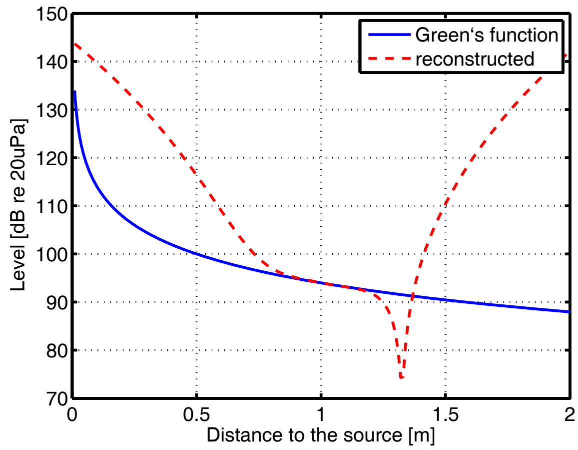

Fig. 5. Sound field generated by a monopole 1 m from the centre of the sphere at $ka = 0.02$. 'True' and reconstructed sound pressure along a line through the monopole and the centre of the sphere.

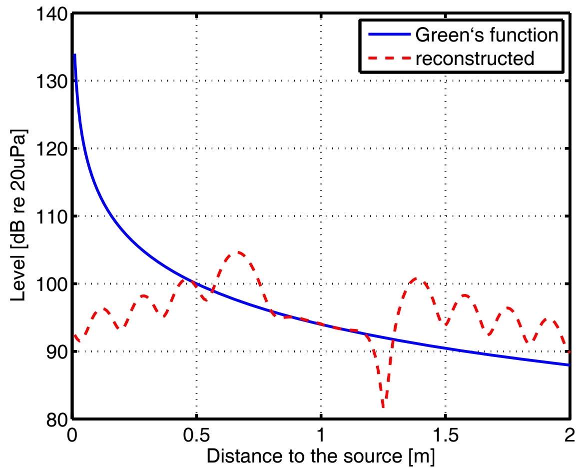

Fig. 6. Sound field generated by a monopole 1 m from the centre of the sphere at $ka = 2$. 'True' and reconstructed sound pressure along a line through the monopole and the centre of the sphere.

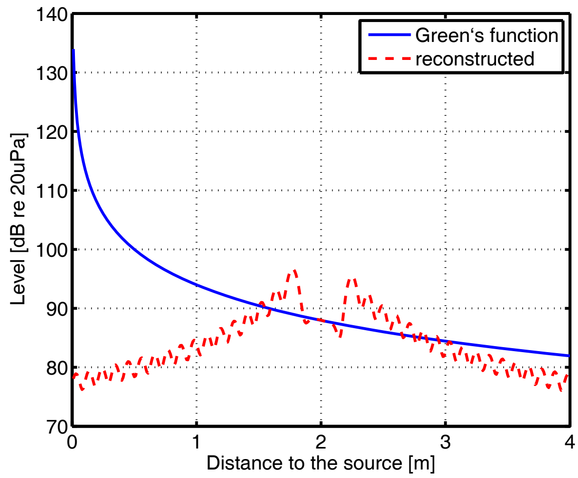

Fig. 7. Sound field generated by a monopole 2 m from the centre of the sphere at $ka = 3$. 'True' and reconstructed sound pressure along a line through the monopole and the centre of the sphere.

Figure 7 shows similar results, but here the monopole is 2 m from the centre of the array and the frequency corresponds to *ka* = 3. Because of the relatively high frequency the reconstruction deteriorates outside the sphere.

Finally Fig. 8 shows an example of reconstructing the interference field generated by two monopoles at a fairly high frequency, *ka* = 5. In this case the reconstruction is only acceptable inside the sphere.

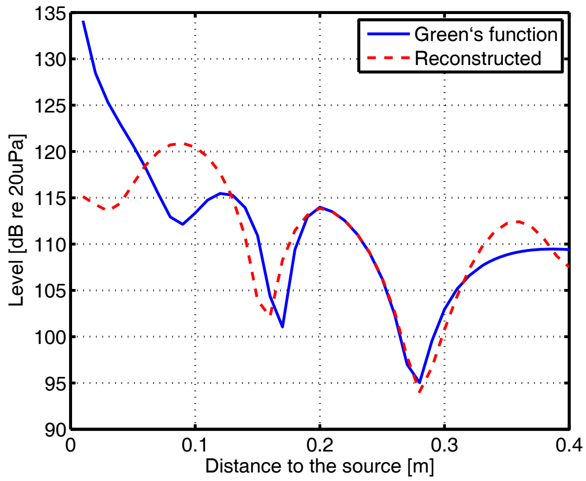

Fig. 7. Sound field generated by two monopoles 20 cm from the centre of the sphere (at different angles) at *ka* = 5. 'True' and reconstructed sound pressure along a line through one of the monopole and the centre of the sphere.

5 Conclusions

Preliminary results from an investigation of spherical near field acoustic holography with fifty microphones flush-mounted on a solid, rigid sphere have been presented. The results indicate that acceptable results can be obtained at distances up to twice the radius of the sphere at frequencies up to *ka* = 2. At frequencies above *ka* = 3 the region of acceptable reconstruction is limited to inside the sphere, and at still higher frequencies even this region is reduced. All in all spherical holography based on a solid sphere seems to give results of similar accuracy as spherical holography based on an open, acoustically transparent sphere does when the sound field is generated by point sources. However, point sources do not reflect sound, and it remains to be seen whether reflections of the backscattered field from the surface of a real source will be a serious problem or not.

References

[1] M. Brandstein and D. Ward (Eds.), *Microphone Arrays. Signal Processing Techniques and Applications*, Springer, Berlin (2001)

[2] J.J. Christensen and J. Hald, 'Beamforming,' *Brüel & Kjær Technical Review* **1** (2004)

[3] B.N. Gover, J.G. Ryan and M.R. Stinson, 'Microphone array system for analysis of directional and spatial variations of sound fields,' *Journal of the Acoustical Society of America* **112**, 1980-1991 (2002)

[4] M. Park and B. Rafaely, 'Sound-field analysis by plane-wave decomposition using spherical microphone array, *Journal of the Acoustical Society of America* **118**, 3094-3103 (2005)

[5] J. Meyers and G.W. Elko, 'A spherical microphone array for spatial sound recordings,' *Journal of the Acoustical Society of America* **111**, 2346 (2002)

[6] J.M. Rigelsford and A. Tennant, 'A 64 element acoustic volumetric array,' *Applied Acoustics* **61**, 469-475 (2000)

[7] E.G. Williams, N. Valdivia and P.C. Herdic, 'Volumetric acoustic vector intensity imager,' *Journal of the Acoustical Society of America* **120**, 1887-1897 (2006)

[8] J. Jourdan and M. Marchall, 'Comparison of beamforming techniques on a sphere,' Department of Electrical Engineering, Technical University of Denmark, Report (2008)

[9] E.G. Williams, *Fourier Acoustics. Sound Radiation and Nearfield Acoustical Holography*, Academic Press, San Diego (1999)

[10] I.H. Sloan and R.S. Womersley, 'Extremal systems of points and numerical integration on the sphere,' *Advances in Computational Mathematics* **21**, 107-125 (2004)